PREPARATION AND INVESTIGATION OF ANTIMONY THIN FILMS FOR MULTI-ALKALI PHOTOCATHODES

X. Liang, M. Ruiz-Osés, I. Ben-Zvi, Stony Brook University, Stony Brook, NY, 11794, USA
S. Schubert, E. Wang, Q. Wu, T. Rao, K. Attenkofer, J. Smedley, BNL, Upton, NY, 11793, USA
J. Wong, H. Padmore, LBNL, Berkeley, CA, 94720, USA
J. Jordan-Sweet. IBM T. J. Watson Research Center, Yorktown Heights, NY, 10598, USA

Abstract

Multialikali antimonide photocathodes exhibit high quantum efficiency in the visible light range, with low thermal emittance and are excellent candidate materials for high average current next generation ERLs or high repetition rate FELs. Although these materials have some excellent characteristics, control of the growth mode of the thin film and ultimately the surface roughness is difficult and will affect the emittance that can be obtained in high gradient fields. Being the first step in multi-alkali photocathode growth, the morphology of Sb films was investigated. X-ray diffraction pole figure (PF) measurement was used to determine the crystallinity of the Sb films. The measurements were complemented by atomic force microscopy (AFM) to determine the roughness and particle size. This study demonstrates how minor changes in deposition rate, thickness and substrate temperature can influence the Sb film properties.

INTRODUCTION

A.H. Sommer discovered that alkali metals such as Sodium (Na), Potassium (K), combined with antimony (Sb) result in photocathodes with high sensitivity and wide spectral response. Although methods for producing high QE films were established long ago, the remaining problems are mainly how to achieve good stoichiometric control so that long wavelength behaviour is reproducible and how to make very smooth films as required for high gradient photoinjectors. A collaboration of Stony Brook University, Brookhaven National Lab and Lawrence Berkeley National Laboratory aims to improve the performance of alkali antimonide photocathodes by using the tools of modern materials techniques such as X-ray diffraction (XRD), grazing incidence small angle X-ray scattering (GI-SAXS), X-ray reflectivity (XRR), AFM and X-ray photoelectron spectroscopy (XPS). [1-5]

This report will focus on recent progress in the analysis of the relationship between evaporation rates, film thickness and roughness.

EXPERIMENTALS

Ex-situ X-ray diffraction pole figure measurement was performed at the National Synchrotron Light Source (NSLS) X20A beam line at Brookhaven National Laboratory (BNL). For the PF measurement, the incident X-ray flux is approximately $8*10^{10}$ photons/second and the energy of the X-rays is 8.05KeV (λ = 1.5406Å). The size of the incident X-ray beam is 0.7 mm high and 0.7mm wide. The incident angle at the center of the linear detector was 20 degrees.

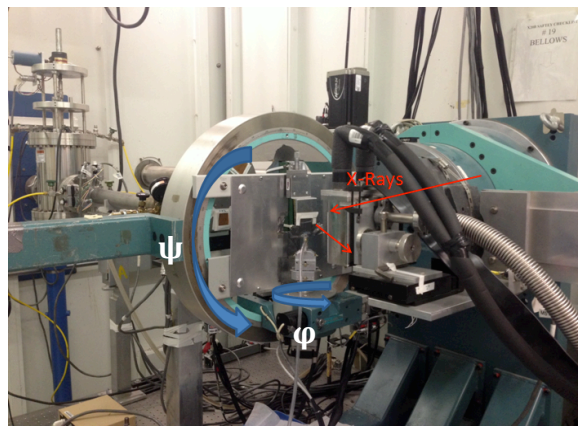

Figure 1: The experimental set up at the X20A beam line at NSLS. The beam line has a 4 circle Huber diffractometer, here just ψ and φ are moveable.

Si (100) wafers were used as the substrate, and all wafers were cleaned using hydrofluoric acid (HF), rinsed in deionized water and dried. The deposition was performed in a UHV chamber with a base pressure of 4×10^{-9} mbar; a Pfeiffer® Prisma QMG 200 residual gas analyzer (RGA) was used to monitored contaminants during growth. Values of H2O never exceeded 5.8×10^{-10} mbar, and CO/CO2 partial pressures were $< 1\times10^{-10}$ mbar during deposition. Deposition rates were monitored using an INFICON® quartz crystal film thickness monitor (FTM).

Surface topography was measured in air over a 1.5 × 1.5 micron area using a Nanosurf® Easyscan 2 AFM with a pyramidal Si (A-CLA mode) probe in BNL building 911 room 210A.

GROWTH PROCESS AND ANALYSIS

Ex-situ XRD PF measurement has been used to characterize the phases and texture changes of Sb thin films. The substrate size of 2cm ×1cm was used. Sb thin films were deposited on these in the UHV chamber by thermal evaporation, with the Sb being evaporated from

*Work supported by the United States Department of Energy through Contract numbers DE-AC02-98CH10886 and at Stony Brook University under Grant No. DE-SC0005713 with the U.S.DOE.
#liangx@bnl.gov

ISBN 978-3-95450-138-0

PtSb beads. To cover a wide range of growth parameters, Sb films were deposited at different evaporation rates at 100C substrate temperature. For each evaporation rate, film thicknesses of 3nm and 10nm were produced; see table 1.

Table 1: Sb Thin Film Sample Preparation

Sample	Evaporation Rate	Thickness
a	0.2Å/s	3nm
b	0.2Å/s	10nm
c	0.4Å/s	3nm
d	0.4Å/s	10nm
e	1Å/s	3nm
f	1Å/s	10nm

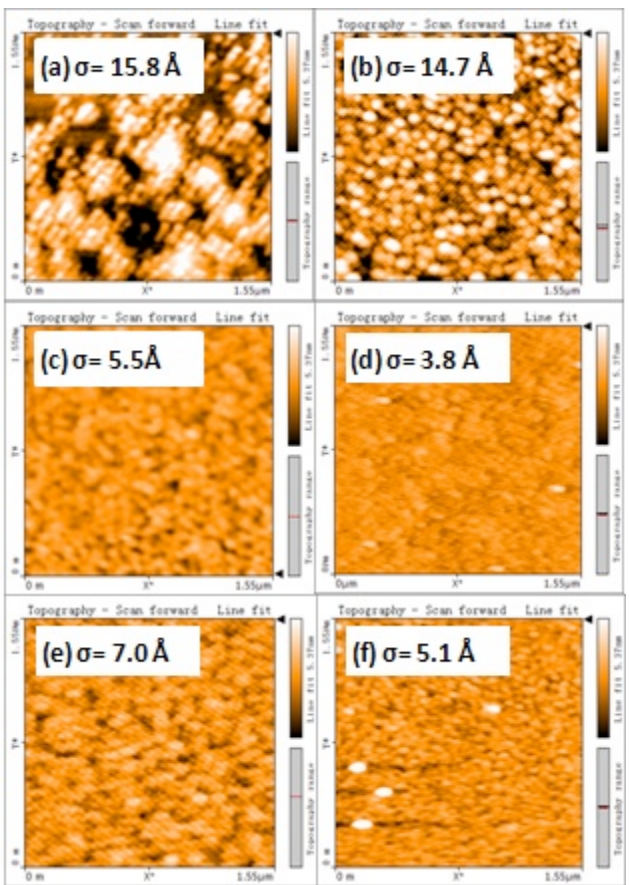

Figure 2: surface topography of six samples. (a) 0.2 Å/s, 3nm , σ=15.8Å;(b) 0.2 Å/s, 10nm, σ=14.6Å; (c) 0.4 Å/s, 3nm, σ=5.5Å; (d) 0.4 Å/s, 10nm, σ=3.8Å; (e) 1 Å/s, 3nm, σ=7.0Å; (f) 1 Å/s, 10nm, σ=5.1Å.

Figure 2 shows the topography and rms roughness of the sample. In general, the highest roughness values were measured for the lowest (0.2Å/s) evaporation rate samples. With the same evaporation rate, thicker films were smoother.

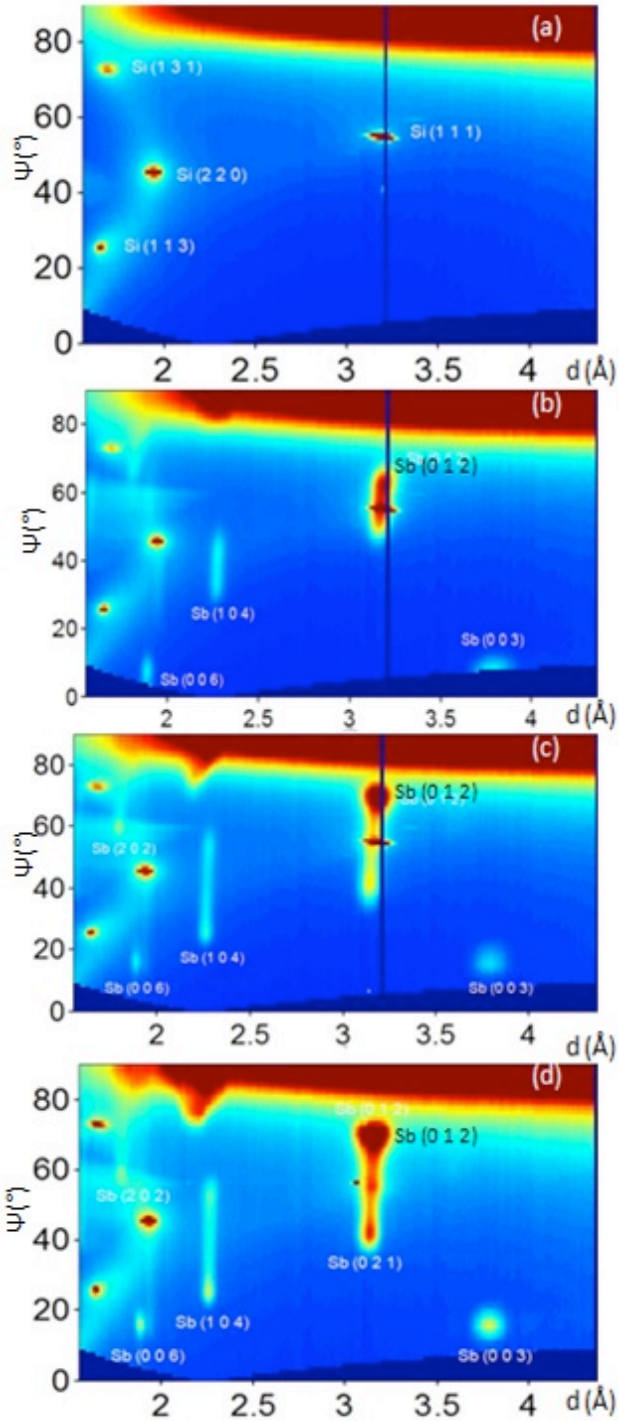

Figure 3: 2D reciprocal space maps; d is the spacing between the planes in the atomic lattice. (a) 0.2 Å/s, 3nm (b) 0.2 Å/s, 10nm; (c) 0.4 Å/s, 10nm; (d) 1 Å/s, 10nm.

The reciprocal space for the Sb films was acquired using radiation with λ=1.5406Å. In these measurements, the incidence angle ω=20° and 2θ=40°. Figure 3 shows the 2D reciprocal space maps. From these graphs, the crystal structure of the thin films can be identified. Figure 3 (a) shows an example of a 3nm Sb film. From this graph, strong Si diffraction peaks were detected. Si (131),

(220), (113) and (111) planes can be identified. No Sb peaks were found from films of this thickness, as their thickness was less than the critical thickness for an amorphous to crystalline transition in this material. Figure 3(b) is for a 10 nm Sb film evaporated at 0.2Å /s corresponding to fig 2 (b); the diffraction peaks for the (012), (003), (006) and (104) planes are visible. (c) 10 nm Sb film evaporated at 0.4 Å /s corresponding to figure 2(d); this is the same as (b) but the (202) and (021) diffraction peaks are present. The intensity of other Sb peaks such as (012) (104) and (003) are increased. The strongest crystalline features are exhibited by the 10 nm Sb film evaporated at 1 Å /s, see figure 3(d); this figure is corresponds to figure 2(f). In figure 3(d), the diffraction intensity of plane Sb(0 12) is the highest.

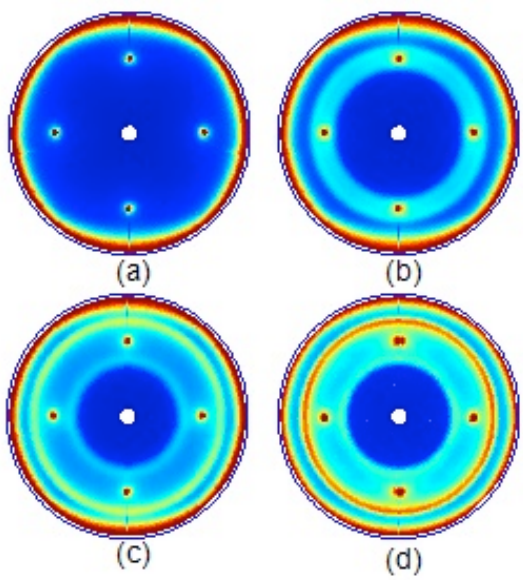

Figure 4: Pole figures of four samples with the same d-spacing. (a) 0.2 Å/s, 3nm; (b) 0.2 Å/s, 10nm; (c) 0.4 Å/s, 10nm; (d) 1 Å/s, 10nm.

Figure 4 presents the pole figure covering a range in d-spacing values from 3.0812 Å to 3.1435 Å. These values cover the Sb (012) peak. (a), (b), (c) and (d) respectively corresponding to figure 3 (a), (b), (c) and (d). The sharp spots in the image correspond to the Si (001) peak. As shown on (a), the background intensity observed is nearly flat and showed no Sb crystalline features. From (b) to (d), the ring structure due to polycrystalline Sb became narrower and sharper, perhaps due to the increase of particle size, though figure 3 makes it clear that there are two (012) orientations present in (c) and (d).

CONCLUDING REMARKS

The evolution of the crystalline structure and topography of Sb films with different evaporation rates and thicknesses at a substrate temperature of 100C has been investigated via X-ray diffraction pole figure and AFM measurements.

AFM measurements indicate the final surface roughness is mainly affected by the evaporation rate. The highest roughness values were measured at the lowest deposition rate of 0.2Å/s. Multi-alkali photocathodes are usually grown from Sb films. In order to avoid a high roughness surface, high deposition rates should be used.

Pole figure measurement shows that the deposition rate affects the crystallinity of the Sb film. The thickness also influences the final texture of the Sb film. When the Sb thickness is small, there is no fiber texture. When approaching a film thickness of 10nm, a significant fiber texture develops.

A wide parameter space still remains to be investigated, such as using different substrate temperatures and a wider range of deposition rates. The specific relationship between the initial Sb layer structure, roughness and the final performance of the cathodes also needs to be determined. Further to this, other sources of roughness will be measured, such as that which results from thin film strain on reaction with K and Cs.

ACKNOWLEDGMENTS

The authors are grateful to Christian Lavoie for his expert assistance. The analysis software used here were written by IBM. Research and experiments were carried out at the National synchrotron Light Source.

REFERENCES

[1] A. H. Sommer, Appl. Phys. Lett. 63, 3(4): p. 62-63.
[2] J. Smedley et al., IPAC 2011, 3206-3208 (2011).
[3] T. Vecchione et al., Appl. Phys. Lett. 99 (2011) 034103.
[4] S. G. Shubert, et al., APL Mater. 1, 032119 (2013).
[5] X. Liang et al., IPAC 2012, 670-672 (2012).

ISBN 978-3-95450-138-0